Chemosphere 244 (2020) 125493

Contents lists available at ScienceDirect

Chemosphere

journal homepage: www.elsevier.com/locate/chemosphere

Zearalenone-induced aberration in the composition of the gut microbiome and function impacts the ovary reserve

Shaojing Tan [a], Wei Ge [b], Junjie Wang [b], Wenxiang Liu [a], Yong Zhao [b], Wei Shen [b], Lan Li [b, *]

[a] College of Animal Science and Technology, Qingdao Agricultural University, Qingdao, 266109, China
[b] College of Life Sciences, Qingdao Agricultural University, Qingdao, 266109, China

HIGHLIGHTS

- Zearalenone disturbs the composition and function of gut microbiome.
- Lysophosphatidylcholines are important for the development of the reproductive system.
- The dysfunction in the gut microbiome after ZEA exposure impacts the ovary reserve.

ARTICLE INFO

Article history:
Received 16 August 2019
Received in revised form
20 November 2019
Accepted 26 November 2019
Available online 29 November 2019

Handling Editor: A. Gies

Keywords:
Zearalenone
Gut microbiome
Lysophosphatidylcholines
Reproductive disorder

ABSTRACT

Zearalenone (ZEA), as a contaminant commonly found in our daily diet, has been widely studied for its toxicity. However, the exact mechanism underlying ZEA induced reproduction disorders remains unclear. Our study aimed to elucidate the underlying relationship between aberrations in the gut microbiota and the degeneration of the ovarian reserve following exposure to ZEA. Four-week-old mice were treated with different doses (0, 20, 40 μg/kg bw/day) of ZEA for 2 weeks and it was found that the primordial follicles were dramatically decreased when compared to untreated controls. Moreover, we applied metagenomic shotgun sequencing to investigate the effects of ZEA exposure on the population composition and function of gut microbiota. The results showed that the abundance of three susceptible bacterial strains, parabacteroides, bacteroides and lachnospiraceae were increased in a dose-dependent manner after ZEA exposure, whereas the bacterial glycerophospholipid metabolism pathway was greatly suppressed. Of note, utilizing LC/MS we found lysophosphatidylcholines (LPCs), important metabolites in the process of glycerophospholipid metabolism, were markedly decreased in the plasma of the ZEA treated mice. In conclusion, our findings here provide evidences that the dysfunction in gut microbiome after ZEA exposure may affect the ovarian reserve.

1. Introduction

In recent years, the worldwide prevalence of mycotoxins produces a major risk factor for human and animal health. According to a survey conducted by Biomin, it is estimated that about 81% of world-wide feed production is contaminated with mycotoxins, including Zearalenone (ZEA) (Rodrigues and Naehrer, 2012). ZEA, also known as F-2 toxin, is a nonsteroidal mycotoxin produced by numerous species of fusarium such as *F. graminearum* and *F. culmorum* (Bennett and Klich, 2003; Bertero et al., 2018). These fusaria usually exist in grains and produce ZEA especially in warm-humid climate conditions. As the structure of ZEA is relatively stable and it is not degraded during harvesting, transportation, storage, or processing. It has been observed that ZEA contamination is found in various food commodities including bread, milled grain products, breakfast cereals, and corn germ oil (Katikou, 2019). ZEA is therefore regarded as a major threat to the food and livestock industry and poses significant risks to human and animal health.

ZEA is a phenolic resorcyclic acid lactone whose chemical construction has similarities with endogenous estrogen (17β-estradiol (E2)). Consequently, ZEA possesses an estrogen-like activity and is able to competitively bind to the cognate receptors (Doll and Danicke, 2011). Therefore, ZEA has been shown to induce dysfunction in the reproductive system in many different species

* Corresponding author.
E-mail addresses: lli@qau.edu.cn, lilan9600@126.com (L. Li).

https://doi.org/10.1016/j.chemosphere.2019.125493
0045-6535/

including mice, pigs, bovine, ovine and horses (Minervini and Dell'Aquila, 2008). There is growing evidence that ZEA can clinically cause hyperestrogenism and reproductive disorders. Swine was reported as the most sensitive animal to ZEA among livestock animals (Gajecki, 2002). Chen et al. reported that ZEA exposure at the dose of 1.1−3.2 mg/kg for 18 days induced endocrine disorders and reproductive toxicity in post-weaning gilts with serum hormone levels and the number of ovarian follicles decreasing in a dose-dependent manner (Chen et al., 2015). ZEA has also been shown to inhibit the maturation of porcine oocytes (Lai et al., 2015). Of particular concern is that ZEA may cause a decrease in the germ cell population during the prenatal periods leading to premature exhaustion of the ovarian reserve. In mice, it was observed that the meiosis progress in female fetal germ cells can be impeded and the formation of the primordial follicle pool disrupted after gravid mice were treated with ZEA (Liu et al., 2017). More importantly, it has been shown that woman's reproductive systems can be affected by a daily diet contaminated with ZEA (Massart et al., 2008). While previous studies provide ample evidence that ZEA exposure leads to reproductive consequences the exact mechanism underlying ZEA induced depletion in the ovarian reserve remains unclear.

The mammalian intestinal canal is the first physical barrier against contaminants in ingested food and contributes to the maintenance of the host physiology. The gut microbiota plays crucial roles in the process of food digestion, general metabolism, immune homeostasis and epithelial function (Blutt et al., 2018). Recently, many studies have implicated the gut microbiota as a leading cause or contributor to many diseases and there is increasing awareness of the harmful effects of toxic substances on the gut microbiota (Avantaggiato et al., 2003). ZEA can be quickly absorbed after oral administration and the gastrointestinal tract is considered the main site of absorption (Saint-Cyr et al., 2013; Guo et al., 2014; Wang et al., 2019). Therefore, the toxic effect of ZEA on the gut microbiome cannot be ignored. Previous work suggests that the signals produced by the gut microbiota have influence on peripheral organs, such as liver (Ma et al., 2017) and brain (Wang and Wang, 2016; Molina-Torres et al., 2019) indicating that the gut microbiota is important in the development and function of these organs. But there is a little evidence showing that the composition of the gut microbiota has an effect on the reproductive system. Recently, it was identified that the bacterial composition in the upper reproductive tract was different between women with and without epithelial ovarian cancer (Rampersaud et al., 2012). Mora et al. found that women with polycystic ovary syndrome (PCOS) had a specific gut microbiota composition compared with normal women (Insenser et al., 2018). These evidences suggest that the gut microbiota has a potential effect on ovarian functions. However, the mechanism of how an imbalance in the gut microbiota affects the reproductive system remains largely unknown.

The possible influence of environmental estrogen on the composition and function of gut microbiota remains unclear. With the advent of high-throughput sequencing techniques, a tool that allows a more comprehensive research of gut microbiome by avoiding laboratory cultivation, plenty of studies illuminate the gut microbiota associations with common diseases (Uritskiy et al., 2018). In the current study we hypothesized that an altered gut microbiota after ZEA exposure may contribute to reproductive disorders due to alterations in bacterial metabolism. Therefore, we utilized metagenomic sequencing to evaluate the influence of ZEA on gut microbiota composition and function, and also to investigate the reproductive toxicity of ZEA exposure on follicular development during early life. We identified a decrease in lysophosphatidylcholines (LPCs) following ZEA exposure which may play a profound role in these two processes. Overall, this study provides us a primary understanding on the microbial effects in the development of the reproductive system.

2. Materials and methods

2.1. Animals, zearalenone exposure, and sample collection

The 4-week-old female CD-1 mice used in our study were obtained from Vital River Co. Ltd. (Beijing, China). A total of 60 mice were divided into 3 groups randomly (20 mice/group, body weight = 26 ± 1 g) and housed separately with ad libitum access to food and water. The animals were kept under standard feeding condition (23 ± 1 °C, 12:12-h light/dark cycle), all operating steps of animal experiments were admitted by the Ethical Committee of Qingdao Agricultural University.

Zearalenone was obtained from Sigma-Aldrich (St.Louis, MO, USA). It was dissolved at a concentration of 40 mg/ml by DMSO (Amersco, Solon, OH, USA), preserved at −20 °C in light-resistant condition, diluted to 20 μg/ml by PBS and stored at 4 °C. In this study, different does of ZEA solution was intragastrically administrated to the mice according to body weight (0, 20, 40 μg/kg bw/day) for 2 weeks, the mice in the control group received the same volume of diluted solution. Two weeks after the final gavage, five mice in each group were randomly selected and the mouse cecum contents were collected into 1.5 ml sterile microcentrifuge tubes separately, then sent to Novogene Co. Ltd. (Beijing, China) at low temperatures quickly after liquid nitrogen flash freezer. Ovarian tissues were fixed in 4% paraformaldehyde solution (Solarbio, Beijing, China). The blood samples were collected and saved in EDTA-containing tubes by means of heart punctures, centrifuged at 1500 rpm for 15 min at - 4 °C, and finally the plasma samples were moved into 1.5 ml sterile microcentrifuge tubes with clear labels and frozen at - 80 °C.

2.2. DNA extraction and metagenomic sequencing

Metagenomic DNA was extracted using the standard protocol of Novogene Co. Ltd. There were about three indicators to evaluate DNA samples quality: purity, concentration and the degree of degradation. After quality control (QC) for DNA, 1 μg DNA in each sample was prepared for generating sequence libraries using NEBNext Ultra DNA Library Prep Kit. First, the DNA sample was fractured to a length of approximately 300 base pairs by ultrasonication, then the DNA fragments were amplified by PCR. Finally, the qualified library preparations were sequenced on an Illumina HiSeq 2500 platform and pair-ended reads were generated for each sample.

2.3. Preprocess of metagenomics sequencing data

A total of 5 samples in each group were used to detect the change in the metagenomic after ZEA exposure. The raw pair-ended data was filtered and trimmed by fastp to trim low-quality bases from the end of the read, then the data was compared with the reference database of mice to remove reads that come from its host, and the clean reads were used in the following analysis process. In this study, we deleted one sample in the control group because it could not provide enough available information.

2.4. Metagenomic assembly and binning

In order to splice the short sequences into long scaftigs/contigs all clean pair-ended fastq data reads were concatenated to one fastq file separately, then we assembled the metagenomic reads with metaWRAP (Uritskiy et al., 2018) - Assembly module. Next, the binning module was used to separate the contig sequences of

different individuals in complex microbial populations, we conducted this process using three different algorithms including MaxBin, CONCOCT, and MaxBin. Then the bin sets were consolidated into a single bin set through strict reassembly to increase the quality of bins set. In this process we selected "-c 90 -x 5" as basic parameters and the accuracy were inspected by CheckM (Parks et al., 2015) database.

2.5. Gene catalogue annotation

Based on sample reads in each group and mixed assembly contigs, we predicted the open reading frames (ORFs) for gene catalogue of 14 samples using PROKKA (Seemann, 2014) pipeline, which could drive the process of locating ORFs and RNA regions on contigs. We mapped clean reads back to the assemblies to quantify the gene in every sample using bowtie 2, it can result in a SAM file, where contained the alignment information. Afterward, the SAM file was changed format to BAM file and sorted, then the BAM files were processed with MarkDuplicates from Picard tool recognized and to get rid of duplicating reads. GFF file was one of several types of output files produced by PROKKA. We used an in-house bash script called prokkagff2gtf.sh searching for gene regions in GFF file. Finally, we employed them to calculate the number of reads mapped to each gene. The relative abundance of the gene was normalized through Transcripts Per Million (TPM) method.

2.6. Bacterial taxonomic annotation

The high-quality reads from each sample were used as input data for MetaPhlAn2 (Truong et al., 2015), a tool to characterize the composition of microbial communities. It is convenient to result in files that contain the list of detected microbes and their relative abundance. The information at each taxonomic level can be extracted by changing the parameters. Then we can compare the relative abundance at each classified level (each level could the sum to 100%). Furthermore, the result of taxonomic profiling was used to create a cladogram with GraPhlAn2 (Asnicar et al., 2015).

2.7. Functional analysis

A GFF file was produced by PROKKA. Firstly, we extracted lists of the genes with enzyme from the GFF file to quantify and compare the abundance of enzymes and metabolic pathways. The MinPath (Ye and Doak, 2009) program was used to get a conservative estimate of the pathways present, and it used two unique input files: a file with gene identifiers and enzyme numbers, separated by tabs, another file that linked each enzyme to one or several pathways. In this study, Metacyc (Caspi et al., 2006) Metabolic Pathway database and Kyoto Encyclopedia of Genes and Genomes (KEGG) database were used to link enzyme information. Furthermore, we used KRONA which could produce HTML files that can be explored interactively.

2.8. Enzyme linked immunosorbent assay (ELISA)

Plasma from each mice was collected to evaluate the relative content of anti-mullerian hormone (AMH), 17 β-estradiol (E2), follicle-stimulating hormone (FSH), and luteinizing hormone (LH) using ELISA kit (Jinma, Shanghai, China) following the manufacturer's instruction. Briefly, the standardy and serum samples were added and adsorbed to wells of an ELISA plate, the enzyme-labeled plate was covered with microplate sealers and incubated at 37 °C for 30 min. Then the wash buffer was used to wash plate for five times (30 s per time), 50 μl horseradish peroxides (HRP)-conjugated reagent was added into each well and incubated at 37 °C for 30 min, After that the plate was washed 5 times again, and each well was added 50 μl TMB substrate A&B solution in turn and incubated at 37 °C for 10 min. Finally, equal volumes of stop solution were added into each well, the absorbance was tested and calculated in 15 min by Multiscan Spectrum (450 nm).

2.9. Histological analysis and histochemical staining

After 2 weeks of ZEA exposure the ovaries were isolated carefully then fixed with 4% paraformaldehyde solution overnight, dehydrated in alcohol gradient, vitrified in by dimethylbenzene and embedded in paraffin. The H&E staining and immunohistochemistry (IHC) staining methods were applied to observe the ovarian morphological features and to detect the development of follicles at each stage in the experimental group following the normalized procedures.

The type and numbers of follicle per ovary were evaluated as previous described (Tilly, 2003). Briefly, the whole ovary was sectioned at 5 μm thickness and distributed in the glass slides evenly, three slides of each ovary were used to calculate the follicle numbers. The follicles were counted every five sections per slide, multiply the mean number of follicles in each slide by the number of slides per ovary to the total number of follicle numbers per ovary.

2.10. The liquid chromatography triple quadrupole tandem mass spectrometry (LC-QQQ-MS/MS) analysis

Three plasma samples in each group were randomly selected and removed from - 80 °C, then defrosted at room temperature. The protein was removed by mixing with the protein precipitator (methanol - acetonitrile (2/1 v/v), ultrasonic in ice water for 10 min and standing 30 min at - 20 °C before centrifuging (10 min, 13,000 rpm, 4 °C). Finally, the supernatant was filtered with 0.22 μm organic pinhole filter and stored in vial at-80 °C before LC/MS analysis.

With Agilent Mass Hunter software (Agilent, USA), the samples were analyzed by using an Agilent 1290 Infinity Binary Pump LC coupled to an Agilent 6400 triple quadrupole MS/MS with Jet Streaming technology and electrospray ionization (ESI). Separation occurred on an AdvanceBio 1.8 μm, 100 × 2.1 mm Zorbax RRHD 300-HILIC (Agilent Technologies) LC column. Data acquisition was performed in Dynamic MRM mode with positive ESI. Special operating source parameters were as follows: The electrospray voltage of capillary was 4.0 kV, the gas temperature was 350 °C, the gas flow rate was 9 l/min, and the nebulizer pressure was 37 psi, Both the sheath gas and auxiliary gas were nitrogen.

2.11. Gene expression analysis

Total RNA was extracted from frozen ovary using an RNAprep pure Micro Kit (Aidlab, RN07, Beijing, China) according to the manufacturer's instructions and then reverse-transcribed into cDNA using TransScript One-Step gDNA Removal and cDNA Synthesis Super Mix (TransGen, AT311-03, Beijing, China). Quantitative real-time PCR (qPCR) was carried out using TB Green™ Premix Ex Taq™ II (TaKaRa, AJ12451A). QPCR primer sequences are shown in Table S1. Gene expression changes were analyzed by the $2^{-\Delta\Delta Ct}$ method and normalized to *Gapdh*.

2.12. Statistical analysis

For metagenomic analysis, all data sets were assessed by one-way analysis of variance (ANOVA) followed by Tukey-Kramer test through STAMP. In addition, other statistical analysis was performed utilizing GraphPad Prism V.8.0.2 (GraphPad Software Inc.,

San Diego, CA, USA). The *P*-value was calculated by paired one-tailed student's t-test, the data were expressed as mean ± SD. All experiments carried at least three times, P value < 0.05 was considered as significantly different, ns indicated no significant different.

3. Results

3.1. ZEA exposure decreased body weight and serum hormone level and induced degeneration in ovarian reserve

To explore the toxic effects of ZEA exposure on female mice we administrated 4-week-old mice with ZEA at doses of 0 (control), 20 μg/kg (low), and 40 μg/kg (high). After 2 weeks daily ZEA intragastric administration we performed histological staining to evaluate the effects of ZEA exposure on female folliculogenesis. We collected the cecum contents for metagenomic sequencing, and collected blood samples for metabolite analysis to explore the impact of ZEA exposure. The whole experimental procedure involved in this study is illustrated in Fig. 1A.

First, we compared the mouse body weight dynamics between the different groups during ZEA treatment. We observed that the body weight in both ZEA-treated groups peaked at about 29.5 g after 9–10 days of ZEA exposure, while the body weight in the control group continued to slowly increase (Fig. 1B). Statistical analysis showed the mouse body weight was prominently decreased in the 40 μg/kg ZEA-treated group compared to that of control group (Fig. 1C). Moreover, to test the toxic effect of ZEA exposure on the mouse ovary we calculated the ratio of ovary weight to body weight but there are no significant differences amongst the three groups (Fig. 1D).

To investigate whether ZEA can serve as an endocrine-disrupting compound (EDC) and disrupt the serum hormone homeostasis leading to accelerated follicle loss, we detected the mouse serum hormone levels after ZEA exposure. We found that the serum hormone levels of AMH, E2, FSH and LH were all decreased in the ZEA-treated groups compared with that of the control group (Fig. 2A). We also observed the morphology of ovaries in the different groups and analyzed the composition of follicles using immunohistochemistry and H&E staining (Fig. 2B and 2C). According to the classification of primordial, primary, secondary and antral follicles, the number of follicles were measured on a per ovary and per slide basis (Fig. 2D and 2E). It is noticeable that the total numbers of primordial follicles were drastically reduced in both ZEA-treated groups compared to that of the control group, indicating that ZEA have a robust harmful effect on the ovarian primordial follicle pool.

3.2. Schematic of annotated phylogenies and taxonomies

To explore the phylogenetic characteristics of cecum bacterial after ZEA exposure we utilized the metagenomic sequencing strategy. There were ~39 million sequencing reads and 13.71 Gb of clean data per sample on average (Fig. S1A). To avoid disturbance from the host DNA we mapped the clean data to the mouse reference genome database and removed the host contamination, the results showed that most of the contamination rates were <50% (Fig. S1B), indicating that our sequence-based profiling method was

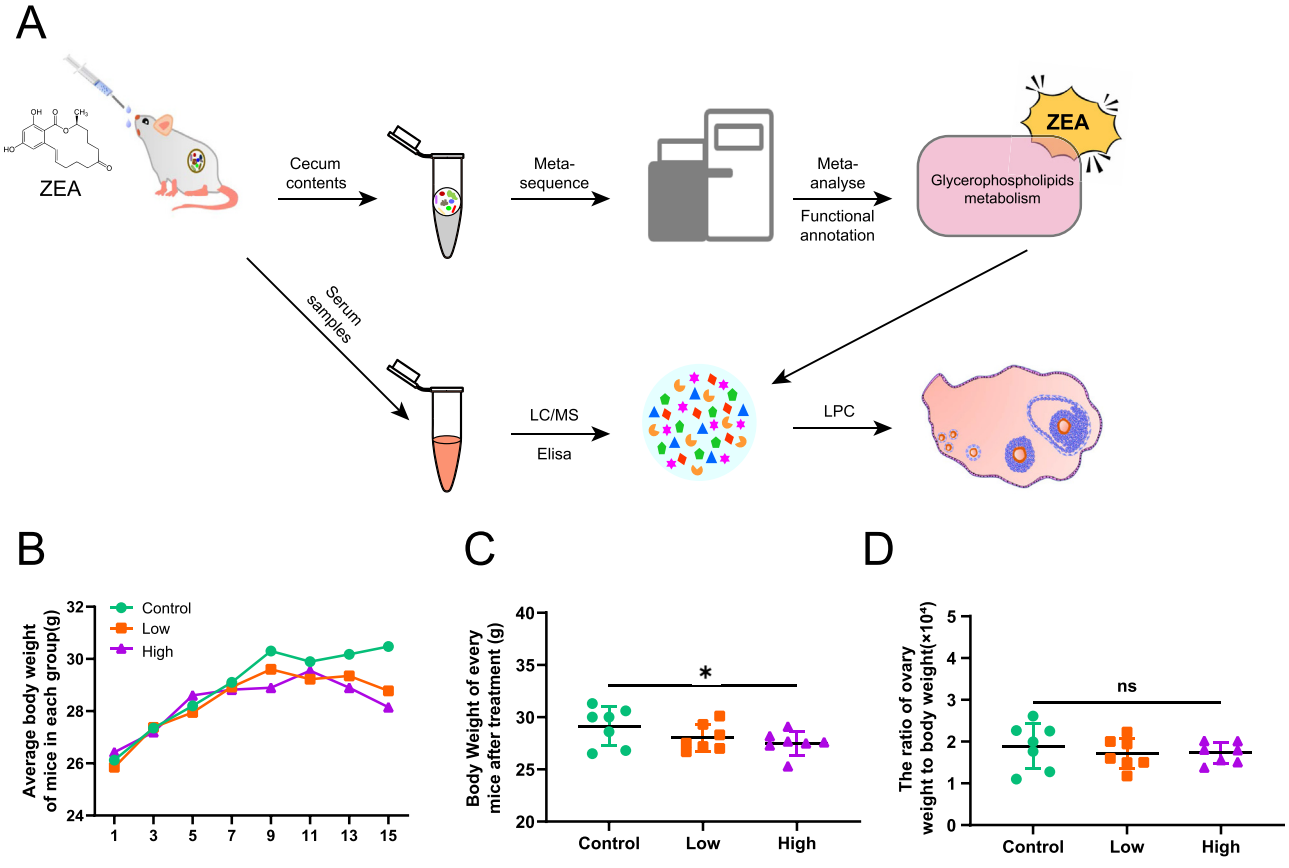

Fig. 1. The schematic of analysis method and phenotypes of mice treated with different dose of ZEA for 2 weeks. (A) Schematic of the experiment design. (B) The change of average body weight in each group during ZEA daily exposure. (C) Body weight of mice in each group after ZEA exposure. (D) The ratio of mice ovary weight to body weight in each group after ZEA exposure. (The mice body weight was measured every two days. *P < 0.05).

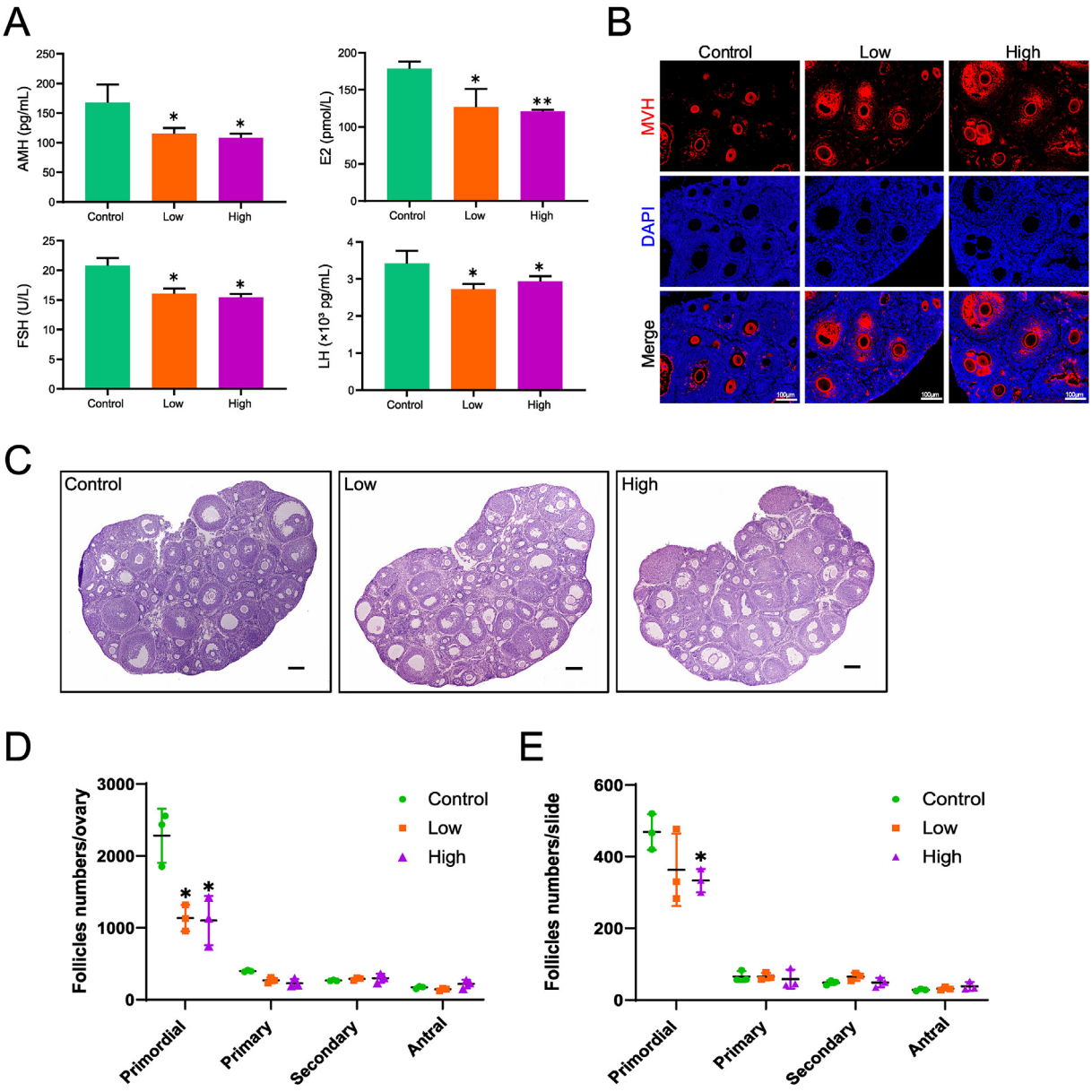

Fig. 2. The decreasing serum hormone level and ovary reservation caused by ZEA. (A) The concentration of AMH, E2, FSH and LH measured by ELISA after ZEA treatment. (B) Nuclear staining (blue) and MVH positive oocytes (red). (C) Representative H&E staining sections of ovaries in each group, Scale bar 50 μm. (D and E) Statistical analysis of the follicle numbers in each experimental group (All experiments carried at least three times; error bars indicate SD. $^{*}P < 0.05$, $^{**}P < 0.01$). (For interpretation of the references to color in this figure legend, the reader is referred to the Web version of this article.)

reliable.

Next, we applied MetaPhlan2 to estimate the composition and structure of the microbial communities from the valid data in each sample and obtained the taxonomic matrix form ranging from kingdoms (Archaea, Bacteria, etc.) to species including relative abundance. Consequently, the taxonomic cladogram was constructed according to the matrix information. The top 100 abundance clades were highlighted in the phylogenetic tree and we found that *bacteroidia* and *firmicutes* were the most abundant at the class level, followed by *bacilli*, *clostridia* and *gammaproteobacterial* (Fig. 3A). The enriched phylum bacteria in the control and ZEA-treated groups were represented in a histogram and we noticed that *proteobacteria* was predominate in the control group, while *firmicutes* in the low dose ZEA-treated group and *bacteroidetes* in the high dose ZEA-treated group (Fig. 3B). Furthermore, principal component analysis (PCA) was performed and demonstrated that the Bray-Curtis distances separated along the second coordinate axis (Fig. S1C). These results indicated that ZEA disturbed the gut bacteria and there existed differences between the low and high dose ZEA-treated groups.

3.3. ZEA exposure induced the changes of cecum microbiome

To gain deeper insight into the microbiome changes after ZEA exposure we extracted the operational taxonomic unit (OUT) equivalents from both species and genus clades. These results showed that the *lactobacillus* and *bacteroides* were two predominant genera across all groups, whereas *escherichia* was only enriched in the control group, and the changed bacteria at species level were consistent with those mentioned above (Fig. 4A and 4B).

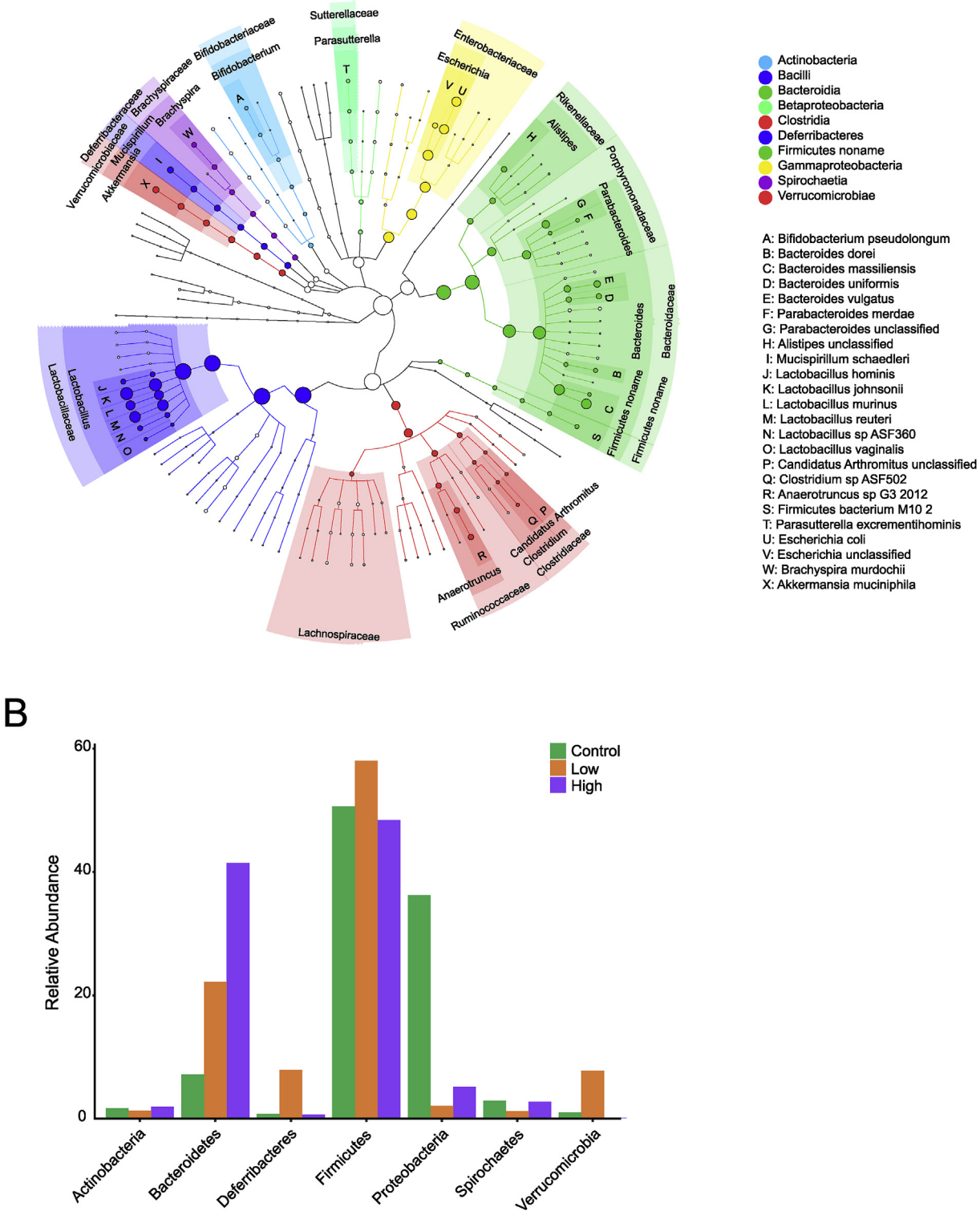

Fig. 3. ZEA changed gut microbiome composition and abundance. (A) Phylogenetic tree of most abundant branches from phyla to species. The origins of bacteria were shown in the inner circle, color-covered areas represent different annotation taxon, and the size of colored dot correspond with relative abundance in each clade. (B) The average abundance of the most common phylum in the three groups. (For interpretation of the references to color in this figure legend, the reader is referred to the Web version of this article.)

The results indicated that ZEA exposure greatly perturbed the composition and abundance of bacterial communities at both the species and genus levels. Next, we observed the distribution of the top 50 in abundance of bacteria at the genus level amongst each group. The results showed that the most abundant bacteria, *lactobacillus*, was enriched in the control group (65%) compared with the low dose ZEA (35%) and high dose ZEA groups (35%), and the total number of enriched bacteria were different amongst the three groups (Fig. 4C). The abundance of the top 25 species was exhibited using a heatmap and the abundance of

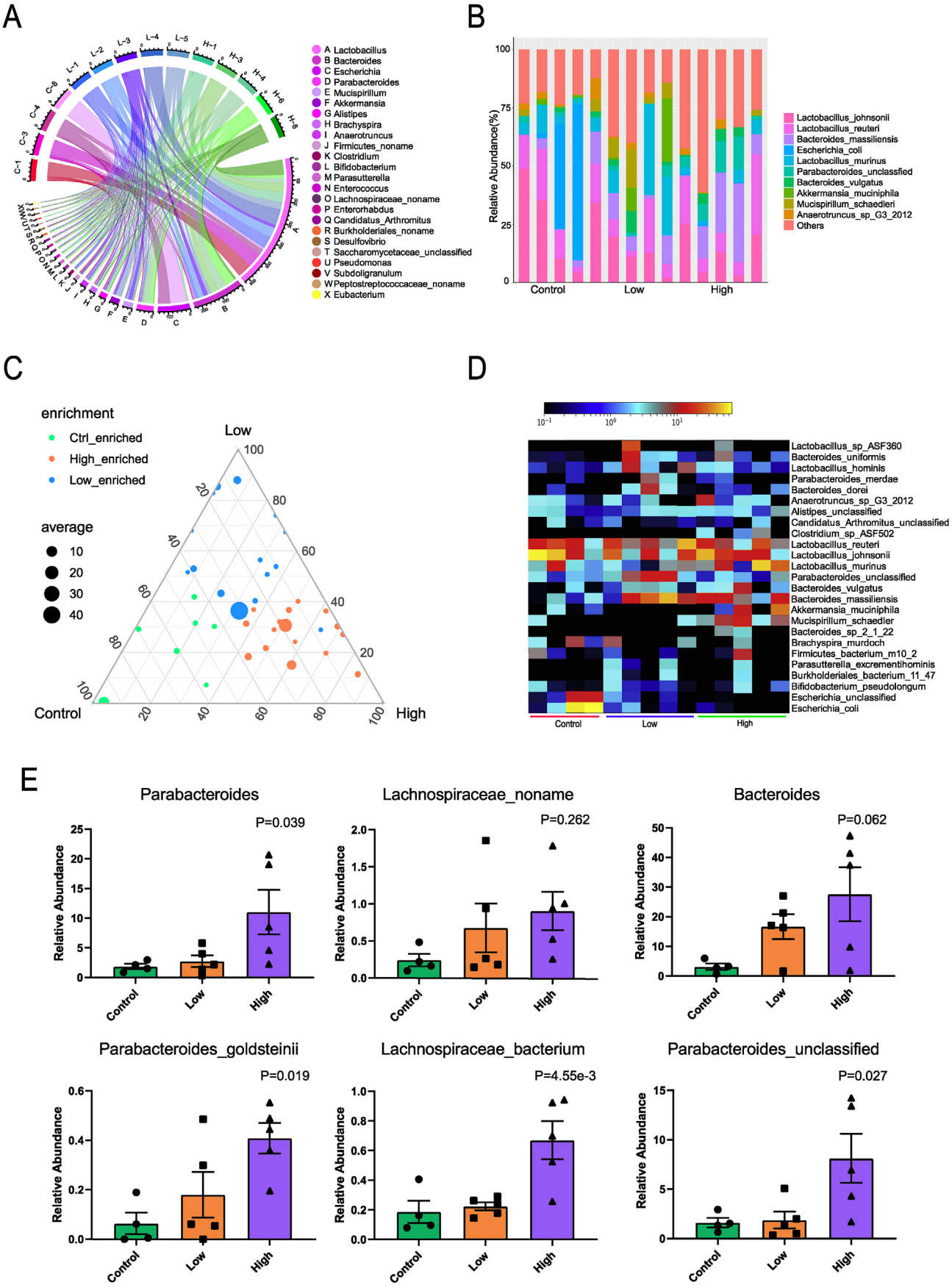

Fig. 4. ZEA altered the cecum microbiome composition profiles at both genus and species level. (A) Chordal graph analysis of the corresponding abundance relationship between samples in each group at the bacterial genus level. (B) The distribution of top 10 abundance microbiome at the bacterial species level. (C) Differential abundant cecum microbiome enriched in the Control, Low, and High groups (each colored-dot represents one kind of bacteria at genus level). (D) Heatmap of differential abundance of taxa at species level among the three groups. (E) The different bacteria at genus (upper) and species (lower) level with *P*-value.

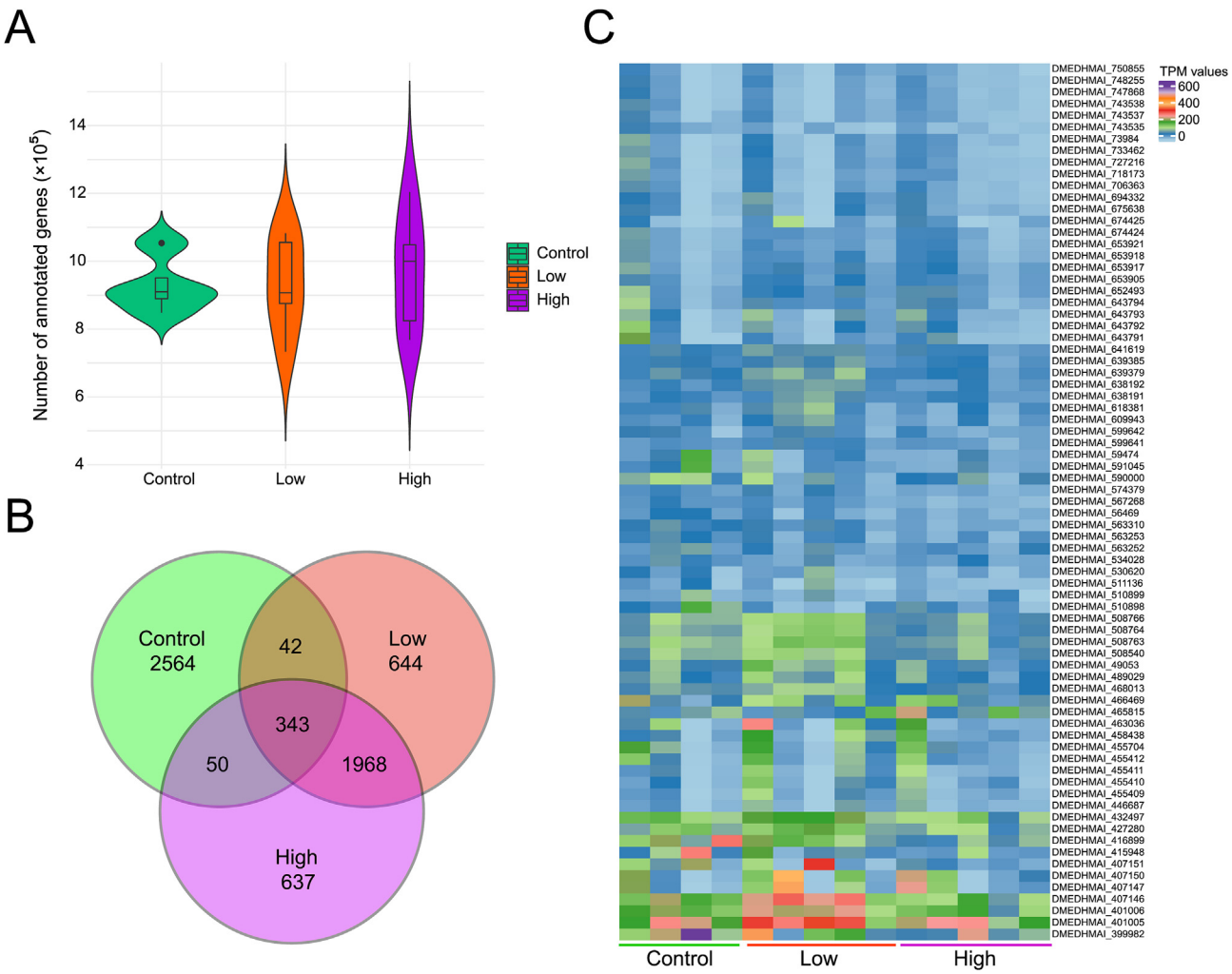

Fig. 5. The gene annotation profiles among three experimental groups. (A) The total number of annotated genes in each sample between three experimental groups. (B) The number of common and specific annotated genes in each group, there were only 385 and 393 genes in low and high group overlapped with control group. (C) The heat map of the relative abundance of top 70/343 common genes among all groups.

Bacteroides_massiliensis, *Parabacteroides_unclassified* and *Bacteroides_vulgatus* were increased in the ZEA-treated groups, whereas several species such as *Escherichia_coli*, *lactobacillus_reuteri* were decreased compared to that of the control group (Fig. 4D). Furthermore, the susceptible bacteria at both genus and species level amongst the three groups were displayed and changed in a dose-dependent manner (Fig. 4E). These results showed that ZEA exposure induced aberrations in the gut microbiome. We also combined the low and high dose ZEA groups as one ZEA treated group and analyzed the significantly different bacteria and found the same result (Fig. S1D).

3.4. ZEA exposure changed the annotated gene profiling

Given the changes of microbial communities after ZEA exposure we next investigated whether the expression of genes related to enzyme synthesis pathways were disturbed amongst the three experimental groups. First, the sequenced short reads were spliced into longer contigs, the assembly results showed that the length less than 6838 accounts for 50% of the total assembly length and the number of contigs reached to 630,254 (Figs. S2A and S2B). The cumulative length and GC content plot also showed the dependability of the assembly results (Figs. S2C and S2D). Then we applied metaWRAP to perform genomes binning after assembly (Fig. S2E), phyla taxonomy of the entire assembled community showed successful binning contigs were different amongst the three groups (Fig. S3A), but the distribution of top 20 abundant genomes showed no difference (Fig. S3B). In addition, we improved the bins with reassembly (Fig. S3C), in which the completion metrics have reached up to 100% (Fig. S3D).

Basing on assembly results a gene catalog was created and quantified according to the assembled contigs and the annotated gene counts were calculated, but we did not observe significant differences of the annotated genes between the groups (Fig. 5A). As for the distribution of the number of genes amongst each group it was obvious that the low and high group shared more genes in common compared to that of the control group, while only 343 genes were overlapped among a total of 3000 genes between all groups (Fig. 5B). The heatmap showed the top 70 most abundance genes among the groups (Fig. 5C). These results revealed that the functional gene catalog of the gut bacteria was significantly altered by ZEA, and the annotated gene abundance was decreased after ZEA treatment.

3.5. ZEA exposure disrupted the functional profiles among different experimental groups

To further investigate the effect of ZEA exposure on the functional profiling, we conducted the enzyme annotations using the KEGG database based on the annotated genes, and the whole classes of energy metabolism pathways were displayed using KRONA. The enzyme annotations from two group (control & high dose ZEA-treated) are displayed in Fig. 6A, and then we made detailed comparisons at each level. First, we analyzed the relative abundance of the main pathways at the first level of KEGG, and our results revealed that the relative pathway abundance declined in the ZEA-treated groups, but only the metabolism pathway showed a significant difference ($P < 0.05$) between the groups (Fig. 6B and C). Then we identified 21 different functional categories at the second level and the abundance was shown with a heat map (Fig. 6D). The results suggested that most of the functional pathways were restrained in the group treated with ZEA. Moreover, to get detailed information about the functional difference between the control, low and high dose ZEA-treated groups, we analyzed the abundance of some important functional pathways at the third level. We found metabolism pathways such as glycerophospholipid metabolism and benzoate degradation were remarkably decreased (Fig. 6E). Overall, our findings indicated that ZEA exposure could significantly affect the function of the intestinal flora.

3.6. ZEA reduced the level of serum LPCs

Phosphatidylcholines is an important metabolite in the glycerophospholipid metabolism pathway, and our previous study had found that the content of LPCs in porcine granulosa cell media was decreased as a result of ZEA exposure (Lai et al., 2018). In the current study, the results showed that the abundance of the glycerophospholipid metabolism pathway was significantly suppressed in ZEA-treated groups (Fig. 6D). Thus, we wondered if the serum LPCs were decreased after ZEA treatment so we utilized LC/MS to detect the relative content of LPCs in the experimental groups. The phospholipids subclasses were provided in the total ion chromatogram (Fig. 7A), and we extracted the ion chromatograms of LPCs from the 18−24 min according to the retention time of standard lipids (Fig. 7B). Three kind of LPCs were extracted with the molecular weights of 496.3 (LPC (16:0)), 524.3 (LPC (18:0)), and 546.3 (LPC (20:3)) (Okudaira et al., 2014). To calculate the relative content of the LPCs in each group the peak area was integrated and the results revealed that there was a significantly depletion in the serum level of LPC (18:0) and LPC (20:3) in mice treated with ZEA (Fig. 7C).

3.7. ZEA impacted the ovarian gene expression involved in the LPC biosynthesis and metabolism

We detected ovarian gene expression involved in the LPC biosynthesis and metabolism process (Fig. 8). The results indicated that the mRNAs encoding enzymes involved in LPC metabolism and catabolism [lysophosphatidylcholine acyltransferase 1/3 (*Lpcat1*), lysophospholipase A1 (*Lyp1a1*)] and group 1 B phospholipase A2 (*Pl2g4a*) were significantly decreased in ZEA-treated mice compared with untreated mice. Similarly, the expression of mRNAs encoding proteins associated with LPC biosynthesis [choline phosphor-transferase 1 (*Chpt1*), and choline kinase β (*Chkβ*)] were significantly decreased in the ZEA-treated mice. In addition, the mRNA encoding the G protein-coupled receptor G2A, which can be activated by LPCs, was also reduced in ZEA-treated mice. The results provide evidence that the host genes were also changed in ZEA-treated mice. However, the exact mechanism underlying ZEA induced reproductive disorders remains unclear. While our metagenomic results showed that the bacterial glycerophospholipid metabolism pathway was greatly suppressed by ZEA, it seems that the effect of gut microbiota can't be ignored.

4. Discussion

To our knowledge this is the first description of the latent relationship between ZEA induced reproductive toxicity and alterations in the gut bacterial populations. In the current study, we observed that the ZEA-induced reduction in primordial follicle numbers had a positive association with the change in body weight and the serum hormones. In addition, the metagenomic sequencing method was applied to identify ZEA induced changes in the gut microbiota. Our results explicitly showed an alteration in the gut microbiota in both low and high ZEA treated groups. We also found that the glycerophospholipid metabolism pathway was suppressed after ZEA exposure. Furthermore, the relative content of serum LPCs, key metabolites in the glycerophospholipid metabolism pathway, were decreased after ZEA exposure compared to the control group. Overall, these results may provide a new insight concerning ZEA exposure leading to aberrations in the gut microbiota and resulting in dysfunction in the reproductive system.

Increasing studies have proved that endocrine-disrupting compounds can affect the development and function of female reproductive system in a wide range of species including humans (Alworth et al., 2002; Adewale et al., 2009). Many evidences have demonstrated that ZEA can act as an endocrine-disrupting agent and induce hormonal disorders and reproductive defects due to its estrogenic like structure (Frizzell et al., 2011). It has been proven that sufficient release and secretion of FSH is important for the maturation of ovarian follicles (Minervini and Dell'Aquila, 2008). Decreased production of FSH and LH leads to reduced granulosa cell steroidogenesis (Rudolph et al., 2016). *In vitro*, it has been shown that ZEA affects steroidogenesis in porcine granulosa cells, resulting in ovarian dysfunction (Zhang et al., 2017b). ZEA exposure has also been shown to suppress the process of folliculogenesis in newborn mice, resulting in a reduction of primordial follicles (Zhang et al., 2017a). In our study, we detected the serum index of AMH, E2, FSH and LH, all of which were decreased in ZEA-treated groups. More importantly, we observed that the number of primordial follicles were drastically reduced in the group treated with ZEA, indicating a robust harmful effect of ZEA on the ovarian reserve.

As dietary ingestion denotes the most common path of human exposure to ZEA, the European Commission has suggested that the tolerable daily intake for zearalenone is 0.25 μg/kg bw/day while the mean levels of human exposure are comprised between 3.0 and 33 μg/kg bw/day for ZEA exposure depending on the grain and grain-based products. Food contaminants and pathogens gain access by passing through the gastrointestinal tract. The gastrointestinal microbiota represents potentially the first target for these toxins. In 2016, Claus et al. reviewed the relationship between the gut microbiota and environmental pollutants, indicating a variety of environmental chemicals (including Polycyclic aromatic hydrocarbons, Nitrotoluenes, Pesticides and Benzene derivatives) can be metabolized by the gastrointestinal microbiota (Claus et al., 2017).

The present study focused on the effect of ZEA on the cecum microbiota by using the whole-genome shotgun sequencing, which provided the overall picture of gut microbial communities and their functions accurately and sensitively. Our findings suggest that Firmicutes and Bacteroidetes were two of the most abundant phyla in the cecum microbiota, consistent with previous studies (Li et al., 2018). We found that the abundance of *parabacteroides* and *bacteroides*, two susceptible genera strains in Bacteroidetes were increased after ZEA exposure compared with the control group.

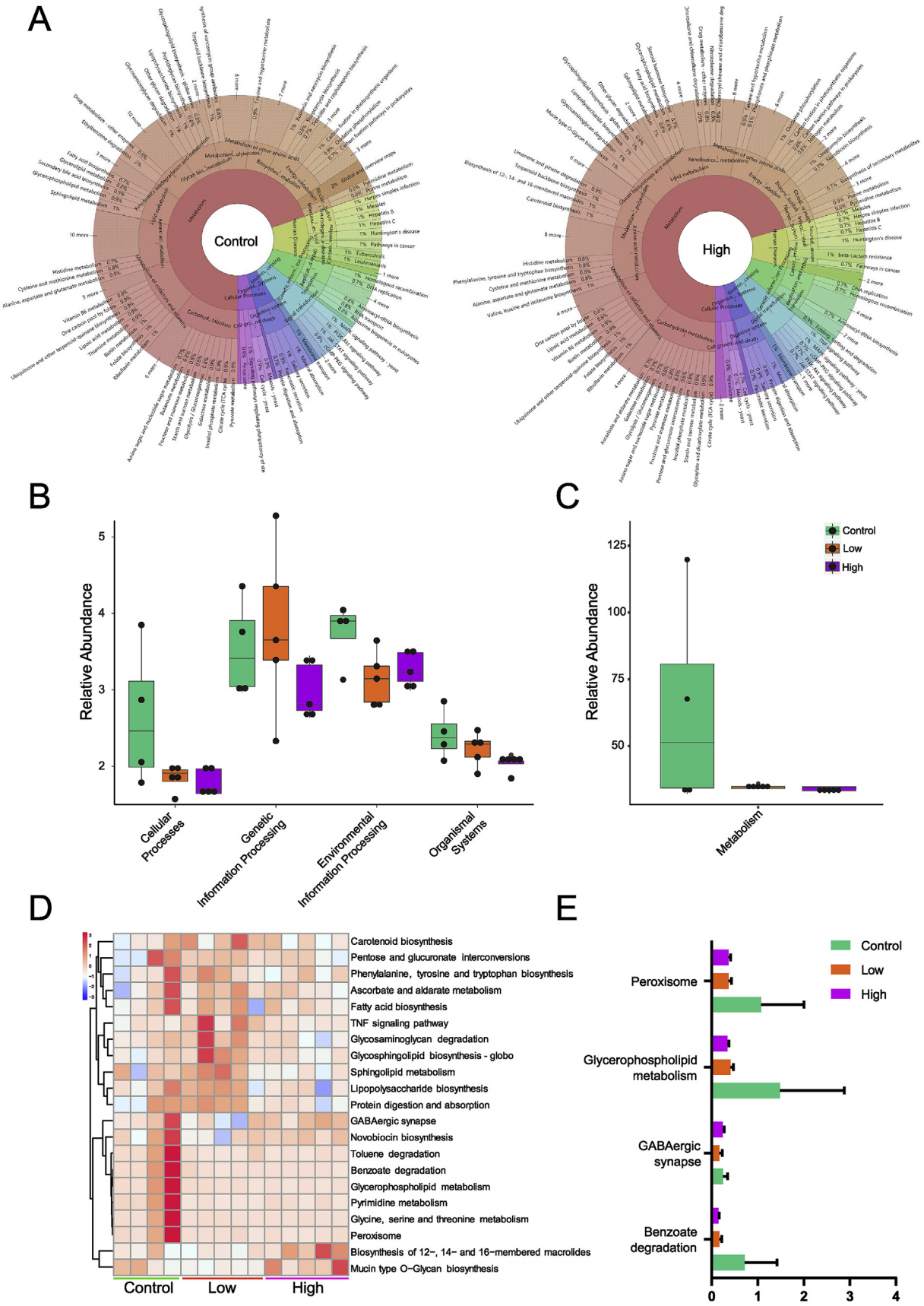

Fig. 6. Metagenomic analysis revealed the KEGG functional profiles of gut bacteria was disrupted by ZEA. (A) The representative KEGG pathways annotation using KRONA between control and high groups. (B and C) Relative abundance of the 5 KEGG pathways in the first classification level, only metabolism pathway showed significantly difference between three groups. (D) The heat map of annotated KEGG pathways at the second classification level. (E) Metabolic pathways with significant differences at the third classification level among three groups.

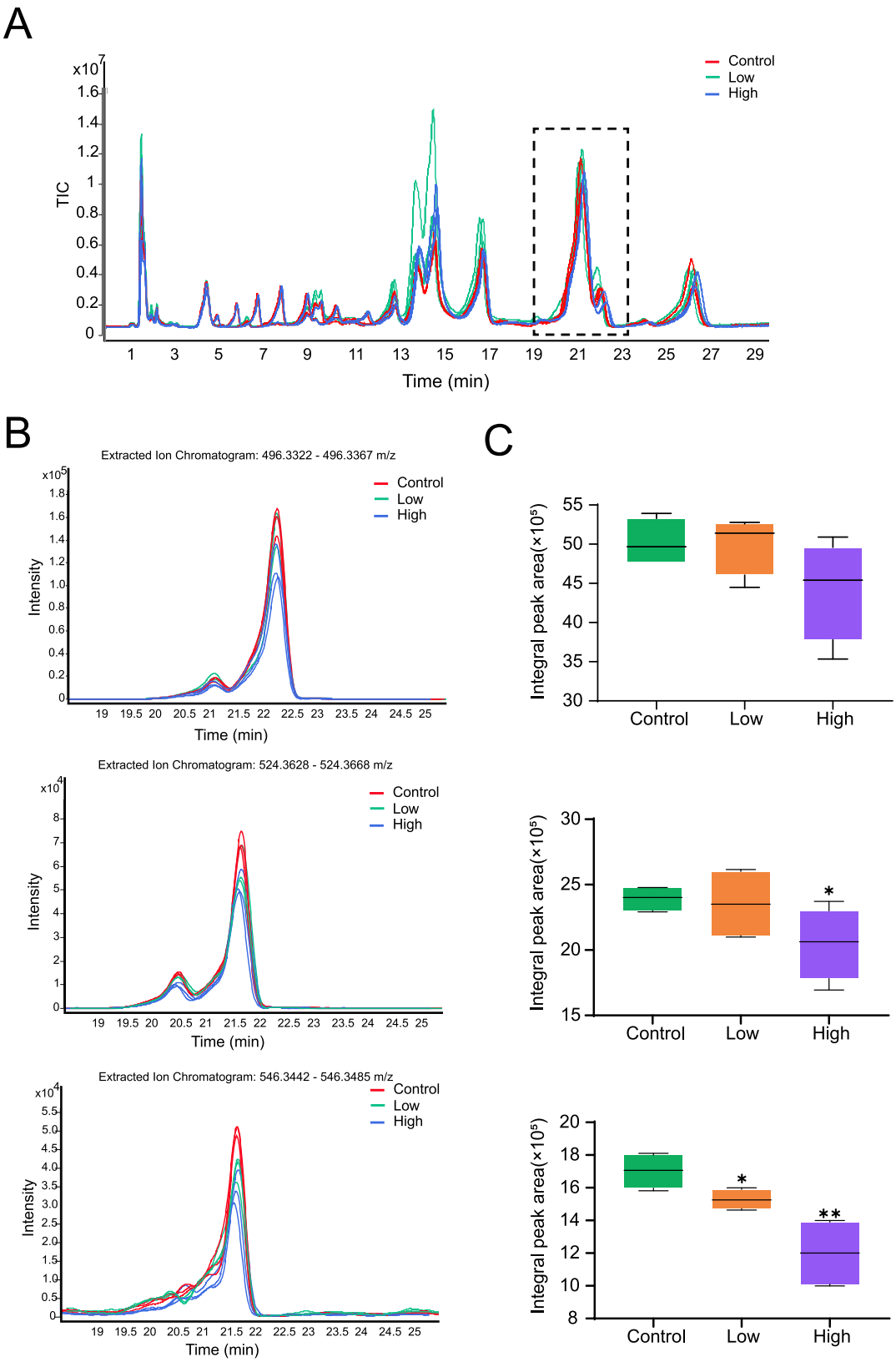

Fig. 7. ZEA reduced the level of serum lyso-phosphatidylcholines (LPCs). (A) Total ion chromatogram profiles among the samples in each group. (B) The signal intensity of three different kind of LPCs with the molecular weights of 496.3, 524.3 and 546.3, respectively. (C) The integral peak area reflected the relative content of the LPCs in each group (All experiments carried at least three times; error bars indicate SD. $^{*}P < 0.05$, $^{**}P < 0.01$).

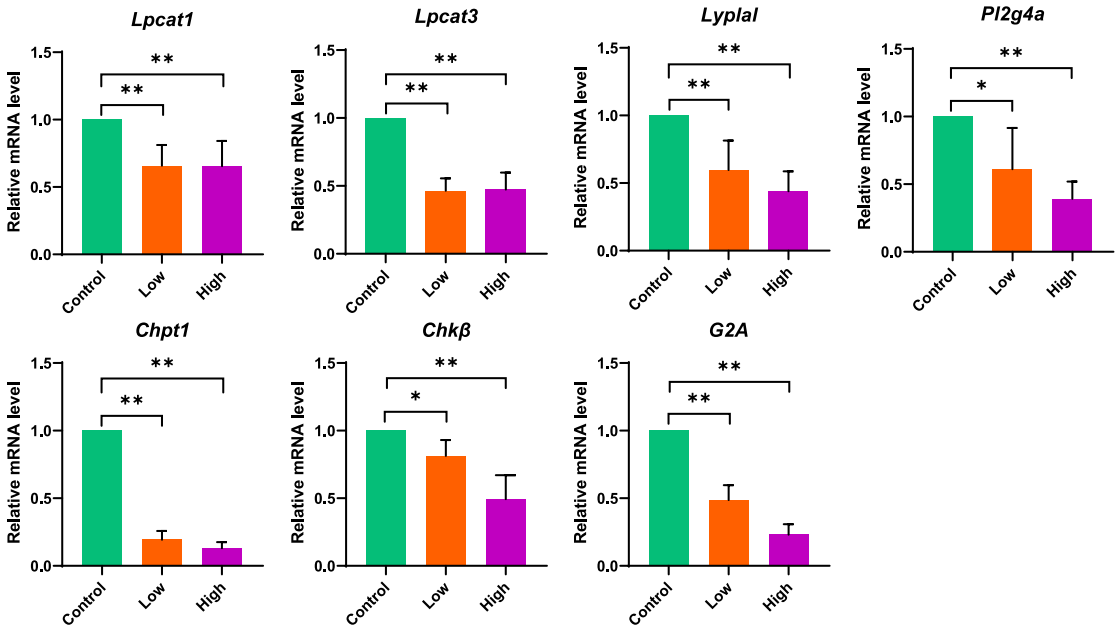

Fig. 8. Ovarian mRNA levels of genes associated with LPC metabolism, catabolism and biosynthesis in mice with two weeks of ZEA treatment (All experiments carried at least three times; error bars indicate SD. $^{*}P < 0.05$, $^{**}P < 0.01$).

Similar with the research of Kondreddy et al., which showed the abundance of rat intestinal *bacteroides* was significantly increased after chronic deoxynivalenol oral gavage (Reddy et al., 2018). In addition, we found that the abundance of *lachnospiraceae* bacterial (phylum Firmicutes) was enriched in ZEA-treated groups. It is noticeable that this kind of bacteria was relatively rare in the normal intestinal tract. However, the abundance of *lachnospiraceae* can be increased by exposure to exogenous chemicals and induced inflammatory diseases (Kameyama and Itoh, 2014; Meehan and Beiko, 2014). Therefore, we hypothesized that ZEA may alter the microbiome composition and induce metabolic disorders.

Recent studies provide evidence that the gastrointestinal microbiota plays a profound role in the physiological functions and pathological processes of human beings. It is therefore likely that a change of composition, diversity or the metabolites produced could have a role in many diseases affecting different organ systems (Schroeder and Backhed, 2016). More recently, it has been found that women with and without PCOS had different gut microbiota communities (Lindheim et al., 2017; Torres et al., 2018), suggesting there may be some connection between the gut microbiota and the ovaries function. Qi et al. reported that Bacteroides *vulgatus* (B.*vulgatus*) was enriched in the gut microbiota of individuals with PCOS, and transplantation experiments indicated that *B. vulgatus* induced disruption of ovarian functions (Qi et al., 2019). According to previous reports, we speculated that the changed microbiota compositions and functions can lead to decreased primordial follicles in the ovary.

From the result of our KEGG pathway annotation we found that the glycerophospholipid metabolism pathway was significantly affected in the groups exposed to ZEA. Dong et al. and Chen et al. applied UPLC-QTOF-MS to investigate the change in metabolic patterns between PCOS patients and controls and found that the levels of lysophosphatidylethanolamines (LPEs) and LPCs were decreased in patients suffering from PCOS (Dong et al., 2015; Chen et al., 2016). Cordeiro et al. found that the follicular fluid lipidomic from aging group was different from the control group, which suggested that aging could affect lipid metabolism and lead to decreased oocyte quality (Cordeiro et al., 2018). In addition, our previous study also demonstrated that LPCs accumulated during follicle growth, but was decreased after ZEA exposure, suggesting that LPCs are crucial for follicular development and oocyte maturation (Lai et al., 2018). In the present study, we detected that serum LPC (16:0) and LPC (20:3) were remarkably decreased in the groups exposed to ZEA compared to the control group.

In this study, we used shotgun metagenomic sequencing to elucidate the impact of ZEA on the gut microbiome and its metabolic functions. The results demonstrated that several susceptible bacterial stains were significantly increased in the ZEA treatment groups. Interestingly, our study found the bacterial metabolic glycerophospholipid metabolism pathway was prominently suppressed after ZEA exposure. Furthermore, the level of LPCs was decreased suggesting a potential relationship with the decreased primordial follicles seen in exposed ovaries. Overall, this study provides new insights to facilitate elucidation of the mechanisms of reproductive toxicity caused by ZEA.

Author contributions

ST, WG and WL conducted the animal experiments; ST and JW analyzed data; ST, WG and JW wrote the manuscript; LL, WS and YZ designed the manuscript. All authors revised the manuscript and approved the final manuscript.

Declaration of competing interest

The authors declare no competing interests.

Acknowledgements

This work was supported by National Key Research and Development Program of China (2016YFD0501207) and National Natural Science Foundation of China (31572225). The authors would like to thank Paul Dyce at Auburn University for his editing of the manuscript.

Appendix A. Supplementary data

Supplementary data to this article can be found online at https://doi.org/10.1016/j.chemosphere.2019.125493.

References

Adewale, H.B., Jefferson, W.N., Newbold, R.R., Patisaul, H.B., 2009. Neonatal bisphenol-a exposure alters rat reproductive development and ovarian morphology without impairing activation of gonadotropin-releasing hormone neurons. Biol. Reprod. 81, 690–699.

Alworth, L.C., Howdeshell, K.L., Ruhlen, R.L., Day, J.K., Lubahn, D.B., Huang, T.H., Besch-Williford, C.L., vom Saal, F.S., 2002. Uterine responsiveness to estradiol and DNA methylation are altered by fetal exposure to diethylstilbestrol and methoxychlor in CD-1 mice: effects of low versus high doses. Toxicol. Appl. Pharmacol. 183, 10–22.

Asnicar, F., Weingart, G., Tickle, T.L., Huttenhower, C., Segata, N., 2015. Compact graphical representation of phylogenetic data and metadata with GraPhlAn. PeerJ 3, e1029.

Avantaggiato, G., Havenaar, R., Visconti, A., 2003. Assessing the zearalenone-binding activity of adsorbent materials during passage through a dynamic in vitro gastrointestinal model. Food Chem. Toxicol. 41, 1283–1290.

Bennett, J.W., Klich, M., 2003. Mycotoxins. Clin. Microbiol. Rev. 16, 497–516.

Bertero, A., Moretti, A., Spicer, L.J., Caloni, F., 2018. Fusarium molds and mycotoxins: potential species-specific effects. Toxins 10.

Blutt, S.E., Crawford, S.E., Ramani, S., Zou, W.Y., Estes, M.K., 2018. Engineered human gastrointestinal cultures to study the microbiome and infectious diseases. Cell Mol Gastroenterol Hepatol 5, 241–251.

Caspi, R., Foerster, H., Fulcher, C.A., Hopkinson, R., Ingraham, J., Kaipa, P., Krummenacker, M., Paley, S., Pick, J., Rhee, S.Y., Tissier, C., Zhang, P., Karp, P.D., 2006. MetaCyc: a multiorganism database of metabolic pathways and enzymes. Nucleic Acids Res. 34, D511–D516.

Chen, X.X., Yang, C.W., Huang, L.B., Niu, Q.S., Jiang, S.Z., Chi, F., 2015. Zearalenone altered the serum hormones, morphologic and apoptotic measurements of genital organs in post-weaning gilts. Asian-Australas. J. Anim. Sci. 28, 171–179.

Chen, Y.X., Zhang, X.J., Huang, J., Zhou, S.J., Liu, F., Jiang, L.L., Chen, M., Wan, J.B., Yang, D.Z., 2016. UHPLC/Q-TOFMS-based plasma metabolomics of polycystic ovary syndrome patients with and without insulin resistance. J. Pharm. Biomed. Anal. 121, 141–150.

Claus, S.P., Guillou, H., Ellero-Simatos, S., 2017. Erratum: the gut microbiota: a major player in the toxicity of environmental pollutants? NPJ Biofilms Microbiomes 3, 17001.

Cordeiro, F.B., Montani, D.A., Pilau, E.J., Gozzo, F.C., Fraietta, R., Turco, E.G.L., 2018. Ovarian environment aging: follicular fluid lipidomic and related metabolic pathways. J. Assist. Reprod. Genet. 35, 1385–1393.

Doll, S., Danicke, S., 2011. The Fusarium toxins deoxynivalenol (DON) and zearalenone (ZON) in animal feeding. Prev. Vet. Med. 102, 132–145.

Dong, F., Deng, D., Chen, H., Cheng, W., Li, Q., Luo, R., Ding, S., 2015. Serum metabolomics study of polycystic ovary syndrome based on UPLC-QTOF-MS coupled with a pattern recognition approach. Anal. Bioanal. Chem. 407, 4683–4695.

Frizzell, C., Ndossi, D., Verhaegen, S., Dahl, E., Eriksen, G., Sorlie, M., Ropstad, E., Muller, M., Elliott, C.T., Connolly, L., 2011. Endocrine disrupting effects of zearalenone, alpha- and beta-zearalenol at the level of nuclear receptor binding and steroidogenesis. Toxicol. Lett. 206, 210–217.

Gajecki, M., 2002. Zearalenone-undesirable substances in feed. Pol. J. Vet. Sci. 5, 117–122.

Guo, M., Huang, K., Chen, S., Qi, X., He, X., Cheng, W.H., Luo, Y., Xia, K., Xu, W., 2014. Combination of metagenomics and culture-based methods to study the interaction between ochratoxin a and gut microbiota. Toxicol. Sci. 141, 314–323.

Insenser, M., Murri, M., Del Campo, R., Martinez-Garcia, M.A., Fernandez-Duran, E., Escobar-Morreale, H.F., 2018. Gut microbiota and the polycystic ovary syndrome: influence of sex, sex hormones, and obesity. J. Clin. Endocrinol. Metab. 103, 2552–2562.

Kameyama, K., Itoh, K., 2014. Intestinal colonization by a Lachnospiraceae bacterium contributes to the development of diabetes in obese mice. Microb. Environ. 29, 427–430.

Katikou, P., 2019. Public health risks associated with tetrodotoxin and its analogues in European waters: recent advances after the EFSA scientific opinion. Toxins 11.

Lai, F.N., Liu, X.L., Li, N., Zhang, R.Q., Zhao, Y., Feng, Y.Z., Nyachoti, C.M., Shen, W., Li, L., 2018. Phosphatidylcholine could protect the defect of zearalenone exposure on follicular development and oocyte maturation. Aging (Albany NY) 10, 3486–3506.

Lai, F.N., Ma, J.Y., Liu, J.C., Wang, J.J., Cheng, S.F., Sun, X.F., Li, L., Li, B., Nyachoti, C.M., Shen, W., 2015. The influence of N-acetyl-l-cysteine on damage of porcine oocyte exposed to zearalenone in vitro. Toxicol. Appl. Pharmacol. 289, 341–348.

Li, P., Yang, S., Zhang, X., Huang, S., Wang, N., Wang, M., Long, M., He, J., 2018. Zearalenone changes the diversity and composition of caecum microbiota in weaned rabbit. BioMed Res. Int. 2018, 3623274.

Lindheim, L., Bashir, M., Munzker, J., Trummer, C., Zachhuber, V., Leber, B., Horvath, A., Pieber, T.R., Gorkiewicz, G., Stadlbauer, V., Obermayer-Pietsch, B., 2017. Alterations in gut microbiome composition and barrier function are associated with reproductive and metabolic defects in women with polycystic ovary syndrome (PCOS): a pilot study. PLoS One 12, e0168390.

Liu, K.H., Sun, X.F., Feng, Y.Z., Cheng, S.F., Li, B., Li, Y.P., Shen, W., Li, L., 2017. The impact of Zearalenone on the meiotic progression and primordial follicle assembly during early oogenesis. Toxicol. Appl. Pharmacol. 329, 9–17.

Ma, J., Zhou, Q., Li, H., 2017. Gut microbiota and nonalcoholic fatty liver disease: insights on mechanisms and therapy. Nutrients 9.

Massart, F., Meucci, V., Saggese, G., Soldani, G., 2008. High growth rate of girls with precocious puberty exposed to estrogenic mycotoxins. J. Pediatr. 152, 690–695, 695 e691.

Meehan, C.J., Beiko, R.G., 2014. A phylogenomic view of ecological specialization in the Lachnospiraceae, a family of digestive tract-associated bacteria. Genome Biol Evol 6, 703–713.

Minervini, F., Dell'Aquila, M.E., 2008. Zearalenone and reproductive function in farm animals. Int. J. Mol. Sci. 9, 2570–2584.

Molina-Torres, G., Rodriguez-Arrastia, M., Roman, P., Sanchez-Labraca, N., Cardona, D., 2019. Stress and the gut microbiota-brain axis. Behav. Pharmacol. 30, 187–200.

Okudaira, M., Inoue, A., Shuto, A., Nakanaga, K., Kano, K., Makide, K., Saigusa, D., Tomioka, Y., Aoki, J., 2014. Separation and quantification of 2-acyl-1-lysophospholipids and 1-acyl-2-lysophospholipids in biological samples by LC-MS/MS. J. Lipid Res. 55, 2178–2192.

Parks, D.H., Imelfort, M., Skennerton, C.T., Hugenholtz, P., Tyson, G.W., 2015. CheckM: assessing the quality of microbial genomes recovered from isolates, single cells, and metagenomes. Genome Res. 25, 1043–1055.

Qi, X., Yun, C., Sun, L., Xia, J., Wu, Q., Wang, Y., Wang, L., Zhang, Y., Liang, X., Wang, L., Gonzalez, F.J., Patterson, A.D., Liu, H., Mu, L., Zhou, Z., Zhao, Y., Li, R., Liu, P., Zhong, C., Pang, Y., Jiang, C., Qiao, J., 2019. Gut microbiota-bile acid-interleukin-22 axis orchestrates polycystic ovary syndrome. Nat. Med. 25 (9), 1459.

Rampersaud, R., Randis, T.M., Ratner, A.J., 2012. Microbiota of the upper and lower genital tract. Semin. Fetal Neonatal Med. 17, 51–57.

Reddy, K.E., Jeong, J.Y., Song, J., Lee, Y., Lee, H.J., Kim, D.W., Jung, H.J., Kim, K.H., Kim, M., Oh, Y.K., Lee, S.D., Kim, M., 2018. Colon microbiome of pigs fed diet contaminated with commercial purified deoxynivalenol and zearalenone. Toxins 10.

Rodrigues, I., Naehrer, K., 2012. A three-year survey on the worldwide occurrence of mycotoxins in feedstuffs and feed. Toxins 4, 663–675.

Rudolph, L.M., Bentley, G.E., Calandra, R.S., Paredes, A.H., Tesone, M., Wu, T.J., Micevych, P.E., 2016. Peripheral and central mechanisms involved in the hormonal control of male and female reproduction. J. Neuroendocrinol. 28.

Saint-Cyr, M.J., Perrin-Guyomard, A., Houee, P., Rolland, J.G., Laurentie, M., 2013. Evaluation of an oral subchronic exposure of deoxynivalenol on the composition of human gut microbiota in a model of human microbiota-associated rats. PLoS One 8, e80578.

Schroeder, B.O., Backhed, F., 2016. Signals from the gut microbiota to distant organs in physiology and disease. Nat. Med. 22, 1079–1089.

Seemann, T., 2014. Prokka: rapid prokaryotic genome annotation. Bioinformatics 30, 2068–2069.

Tilly, J.L., 2003. Ovarian follicle counts-not as simple as 1, 2, 3. Reprod. Biol. Endocrinol. 1, 11.

Torres, P.J., Siakowska, M., Banaszewska, B., Pawelczyk, L., Duleba, A.J., Kelley, S.T., Thackray, V.G., 2018. Gut microbial diversity in women with polycystic ovary syndrome correlates with hyperandrogenism. J. Clin. Endocrinol. Metab. 103, 1502–1511.

Truong, D.T., Franzosa, E.A., Tickle, T.L., Scholz, M., Weingart, G., Pasolli, E., Tett, A., Huttenhower, C., Segata, N., 2015. MetaPhlAn2 for enhanced metagenomic taxonomic profiling. Nat. Methods 12, 902–903.

Uritskiy, G.V., DiRuggiero, J., Taylor, J., 2018. MetaWRAP-a flexible pipeline for genome-resolved metagenomic data analysis. Microbiome 6, 158.

Wang, H.X., Wang, Y.P., 2016. Gut microbiota-brain Axis. Chin. Med. J. 129, 2373–2380.

Wang, J.J., Zhang, R.Q., Zhai, Q.Y., Liu, J.C., Li, N., Liu, W.X., Li, L., Shen, W., 2019. Metagenomic analysis of gut microbiota alteration in a mouse model exposed to mycotoxin deoxynivalenol. Toxicol. Appl. Pharmacol. 372, 47–56.

Ye, Y., Doak, T.G., 2009. A parsimony approach to biological pathway reconstruction/inference for genomes and metagenomes. PLoS Comput. Biol. 5, e1000465.

Zhang, G.L., Sun, X.F., Feng, Y.Z., Li, B., Li, Y.P., Yang, F., Nyachoti, C.M., Shen, W., Sun, S.D., Li, L., 2017a. Zearalenone-exposure impairs ovarian primordial follicle formation via down-regulation of Lhx8 expression in vitro. Toxicol. Appl. Pharmacol. 317, 33–40.

Zhang, G.L., Zhang, R.Q., Sun, X.F., Cheng, S.F., Wang, Y.F., Ji, C.L., Feng, Y.Z., Yu, J., Ge, W., Zhao, Y., Sun, S.D., Shen, W., Li, L., 2017b. RNA-seq based gene expression analysis of ovarian granulosa cells exposed to zearalenone in vitro: significance to steroidogenesis. Oncotarget 8, 64001–64014.